Comparison of Heteronuclear Coupling Constants for Isostructural Nitrogen Coordination Compounds of $^{111/113}$Cd and ^{199}Hg

Deborah C. Bebout* and Sarah W. Stokes

Department of Chemistry, The College of William and Mary, Williamsburg, Virginia 23187

Raymond J. Butcher

Department of Chemistry, Howard University, Washington, DC 20059

Received July 15, 1998

The complexation of Cd(II) by the tripodal ligand tris[(2-pyridyl)methyl]amine and dipodal ligand bis[(2-pyridyl)-methyl]amine was investigated by solution-state NMR and X-ray crystallography. Cadmium coordination compounds exhibiting rarely observed solution-state NMR ^{1}H−$^{111/113}$Cd satellites were characterized. The eight-coordinate complex $[Cd(TMPA)_2](ClO_4)_2$·toluene (**1**) crystallizes in the triclinic space group $P\bar{1}$ with $a = 9.629(2)$ Å, $b = 11.020(2)$ Å, $c = 11.641(2)$ Å, $\alpha = 114.069(13)°$, $\beta = 97.492(13)°$, $\gamma = 91.034(14)°$, and $Z = 1$. The average Cd−N_{amine} distance is 2.53(4) Å and the average Cd−$N_{pyridyl}$ distance is 2.54(6) Å. The complex $[Cd(BMPA)(NCCH_3)(OH_2)(OClO_3)][Cd(BMPA)_2](ClO_4)_3$·$(CH_3CN)$ (**2**) crystallizes in the triclinic space group $P\bar{1}$ with $a = 10.446(2)$ Å, $b = 16.653(3)$ Å, $c = 17.736(3)$ Å, $\alpha = 62.479(9)°$, $\beta = 80.606(14)°$, $\gamma = 84.66(2)°$, and $Z = 2$. In the pseudo-octahedral monocation, the nitrogen-containing ligands occupy equatorial positions with Cd−N distances of 2.321(8), 2.283(7), and 2.263(8) Å for the amine, pyridyl (average) and acetonitrile nitrogens, respectively. Significant axial interactions occur with Cd−O bond distances of 2.313(7) Å (water) and 2.478(7) Å (perchlorate). In the pseudo-trigonal prismatic dication, the average Cd−N_{amine} distances is 2.395(5) Å and the average Cd−$N_{pyridyl}$ distance is 2.362(8) Å. The solid-state structures and solution-state NMR trends were very similar to recently reported isovalent complexes of Hg(II), providing an exceptional opportunity to compare coupling constants of coordination compounds. Implications for the use of $^{111/113}$Cd and ^{199}Hg NMR as metallobioprobes are discussed.

Introduction

Structural characterization of the local metal coordination sites of metallobiopolymers is essential for understanding their function. Recent proposals of new classes of metal binding motifs to biopolymers entices further development of methods which can provide information about metal coordination environments.[1] NMR is one of the few techniques that can directly address the structure of complex biomolecules. Unfortunately, none of the physiologically essential transition metal ions possesses isotopes with favorable NMR properties. For three decades, ^{113}Cd NMR has proved valuable in the characterization of protein metal-binding sites, particularly for zinc and calcium metalloenzymes.[2] Recently, evidence suggesting that ^{199}Hg NMR could also be a valuable structural metallobioprobe has been presented.[3−6]

Cadmium and mercury are in the same periodic family but possess complementary coordination preferences. Cadmium prefers harder ligands such as oxygen while mercury prefers softer ligands such as sulfur. Protein metal binding sites typically contain three to six oxygen, nitrogen, and/or sulfur donors depending on the identity of the native metal ion and its function. The tertiary structure of the protein imposes a specific orientation on the donor atoms which serves to both enhance selectivity for the correct metal ion and provide the appropriate electronic environment to facilitate the desired chemistry. Both Cd(II) and Hg(II) are d^{10} metal ions with low coordination geometry preferences. As a result, both metals can readily replace and subsequently adopt the coordination environment of the native metal ion in many proteins.[2−7]

Mercury has two NMR active isotopes. ^{199}Hg has spin $I = {}^1/_2$, natural abundance 16.84%, and receptivity 5.42 times greater than ^{13}C while ^{201}Hg is quadrupolar and not routinely detectable. Both NMR active isotopes of cadmium have spin $I = {}^1/_2$. ^{113}Cd has a natural abundance of 12.26% and is typically used in direct observe experiments because its receptivity (7.59 compared to carbon) is greater than that of ^{111}Cd (natural abundance 12.75%,

(1) (a) Lippard, S. J.; Berg, J. M. *Principles of Bioinorganic Chemistry*; University Science: Mill Valley, CA, 1994. (b) Schwabe, J. W. R.; Klug, A. *Nat. Struct. Biol.* **1994**, *1*, 345. (c) Karlin, K. D. *Science* **1993**, *261*, 701. (d) O'Halloran, T. V. *Science* **1993**,*261*, 715.

(2) For reviews see: (a) Coleman, J. E. *Methods Enzymol.* **1993**, *227*, 16. (b) Summers, M. F. *Coord. Chem. Rev.* **1988**, *86*, 43. (c) Ellis, P. D. *Science* **1983**, *221*, 1141.

(3) Utschig, L. M.; Bryson, J. W.; O'Halloran, T. V. *Science* **1995**, *268*, 380.

(4) Blake, P. R.; Lee, B.; Summers, M. F.; Park, J.-B.; Zhou, Z. H.; Adams, M. W. W. *New J. Chem.* **1994**, *18*, 387.

(5) Utschig, L. M.; Wright, J. G.; Dieckmann, G.; Pecoraro, V.; O'Halloran, T. V. *Inorg. Chem.* **1994**, *34*, 2497.

(6) Utschig, L. M.; Baynard, T.; O'Halloran, T. V. *Inorg. Chem.* **1997**, *36*, 2926.

(7) (a) Marmorstein, R.; Carey, M.; Ptashne, M.; Harrison, S. C. *Nature* **1992**, *356*, 408. (b) Church, W. B.; Guss, J. M.; Freeman, H. C. *J. Biol. Chem.* **1986**, *261*, 234−237.

10.1021/ic980825y CCC: $18.00
Published on Web 02/24/1999

receptivity 6.92 compared to carbon). The chemical shift anisotropy associated with the ^{199}Hg nucleus is typically significantly larger than that associated with ^{113}Cd.[8] However, with respect to several other NMR parameters, ^{199}Hg appears to have some distinct advantages over ^{113}Cd as a structural metallobioprobe.[3] First, the shorter relaxation times for ^{199}Hg allow for a more rapid rate of data accumulation in direct-observe experiments. Second, ^{199}Hg has a greater chemical shift dispersion which results in greater variation with geometry, ligand type and coordination number. Finally, the strong coupling of ^{199}Hg to side chain proton-spin systems has permitted coherence transfer methods to be applied to a metalloprotein 5-fold larger than any reported in ^{1}H{^{113}Cd} heteronuclear multiple quantum coherence (HMQC) experiments.[3] In this work, we provide evidence that ^{199}Hg may generally couple more strongly than ^{113}Cd to the protons of nitrogen-based ligand systems.

We recently structurally characterized several small coordination compounds of Hg(II) with the multidentate nitrogen ligands tris[(2-pyridyl)methyl]amine (TMPA) (**3**)[9] and bis[(2-pyridyl)-methyl]amine (BMPA) (**4**).[10] These and related dipodal and

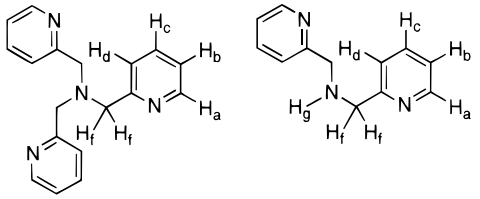

3 **4**

tripodal ligands have been applied extensively to the synthesis of metal complexes because of their ease of preparation and their ability to model the steric and electronic features of protein metal binding sites. There is a wealth of spectroscopic and X-ray crystallographic data available for the metal complexes of **3** and **4** which suggests that essentially isostructural complexes of Cd(II) and Hg(II) should be isolable with these ligands. In this work, we compare the X-ray structures of Cd(II) complexes of **3** and **4** to the Hg(II) complexes we isolated previously. In addition, we report solution-state ^{1}H NMR chemical shift trends for these ligands as a function of the Cd(II)-to-ligand ratio which are similar to the previously reported data for Hg(II). Despite the apparent similarity between the solution- and solid-state structures of the complexes of these two metals, substantial differences in the magnitudes of their heteronuclear coupling constants to ligand protons were observed. The theoretical foundations for these large differences are explored and the implications for application of ^{113}Cd and ^{199}Hg NMR as structural metallobioprobes are discussed.

Experimental Section

Methods and Materials. Starting materials were of commercially available reagent quality from Acros, Aldrich, or TCI America. FT-IR spectra were recorded in KBr pellets on a Perkin-Elmer 1600. Elemental analyses were carried out by Atlantic Microlab, Inc. (Norcross, Ga).

All of the perchlorate salts of Cd(II) and Hg(II) complexes discussed in this work were stable for routine synthesis and purification procedures. *However, caution should be exercised because perchlorate salts of metal complexes with organic ligands are potentially explosive.*[11]

Synthesis of the Complex [Cd(TMPA)$_2$](ClO$_4$)$_2$·toluene (1). The ligand TMPA was prepared by variation of the procedure described by Tyeklár and co-workers as previously described.[9] A solution of Cd(ClO$_4$)$_2$·6H$_2$O (61 mg, 145 μmol) in 2 mL acetonitrile was added to a solution of the ligand TMPA (101 mg, 350 μmol) in acetonitrile (3 mL) with stirring. The solution was diluted with approximately 5 mL of toluene. Colorless plates of the complex suitable for X-ray diffraction analysis formed after several days of slow evaporation. Mp: 232−238 °C (dec). ^{1}H NMR (CD$_3$CN, 20 °C, 2 mM): δ 7.74 (ddd, 6 H, J = 1, 8, 8 Hz, H$_c$), 7.47 (d, J = 4 Hz, 6 H, H$_a$), 7.42 (t, 6 H, J = 8 Hz, H$_d$), 6.84 (dd, J = 5, 8 Hz, 6 H, H$_b$), 4.28 (s, J(HHg) = 8 Hz, 12 H, H$_f$). IR (KBr, cm^{-1}): 2959 w, 2930 w, pyridine C−H; 1601 s, 1573 m, py C═N; 1480 m, 1438 m, pyridine C═C; 1091 vs, ClO$_4$; 2872 w, 2857 w, 1733 m, 1728 m, 1375 w 1349 w, 1308 w, 1288 m, 1272 m, 1262 m, 1153 m, 1053 m, 1009 m, 1002 m, 907 m, 837 m, 775 m, 761 s, 738 m, 623 s. Anal. Calcd for C$_{43}$H$_{44}$CdCl$_2$N$_8$O$_8$: C, 52.48; H, 4.51; N, 11.39. Found: C, 52.38; H, 4.40; N, 11.36.

Synthesis of the Complex [Cd(BMPA)(NCCH$_3$)(OH$_2$)(OClO$_3$)]-[Cd(BMPA)$_2$](ClO$_4$)$_3$·(CH$_3$CN) (2). A solution of the ligand BMPA (100 mg, 502 μmol) in 2 mL acetonitrile was added to an acetonitrile solution (2 mL) of Cd(ClO$_4$)$_2$·6H$_2$O (155 mg, 370 μmol) with stirring. The solution was diluted with 4 vol of toluene. The complex (108 mg, 85% yield) formed as colorless crystals suitable for X-ray diffraction analysis by slow evaporation. Mp: 224−228 °C. ^{1}H NMR (CD$_3$CN, 2 mM, primed protons associated with 1:1 metal-to-ligand cation): δ 8.59 (d, 2 H, J = 5 Hz, J(HHg) = 9 Hz, H$_a$′), 8.02 (ddd, 6 H, J = 2, 8, 8 Hz, H$_c$), 7.88 (d, 4 H, J = 4 Hz, J(HHg) = 6 Hz, H$_a$), 7.56 (d, 4 H, J = 7 Hz, H$_d$), 7.54 (dd, 2 H, J = 8, 2 Hz, H$_b$′), 7.47 (d, 2 H, J = 7 Hz, H$_d$′), 7.38 (dd, 4 H, J = 7, 5 Hz, H$_b$), 4.37 (m, 6 H, H$_f$ + H$_f$′), 3.96 (m, 4 H, H$_f$), 4.85 (m, 2 H, H$_f$′). IR (KBr, cm^{-1}): 3077 w, 3032 w, pyridine C−H; 1604 s, 1573 m, py C═N; 1484 m, 1439 s, pyridine C═C; 1160 vs, ClO$_4$; 1369 m, 1313 m, 1292 m, 1262 m, 1221 m, 1017 m, 1007 sh, 969 w, 945 w, 911 m, 891 sh, 841 w, 810 w, 766 s, 747 m, 731 w, 700 w, 656 w, 624 s. Anal. Calcd for C$_{40}$H$_{47}$Cd$_3$Cl$_4$N$_{11}$O$_{17}$: C, 36.38; H, 3.59; N, 11.67. Found: C, 36.95; H, 3.55; N, 11.14.

Synthesis of the Complex [Cd(BMPA)$_2$](ClO$_4$)$_2$·0.5toluene (5). A solution of the ligand BMPA (158 mg, 793 μmol) in 2 mL acetonitrile was added to an acetonitrile solution (2 mL) of Cd(ClO$_4$)$_2$·6H$_2$O (245 mg, 796 μmol) with stirring. The solution was diluted with two volumes of toluene. The complex formed as colorless crystals by slow evaporation. Mp: 224−226 °C. ^{1}H NMR (CD$_3$CN, 2 mM, 20 °C): δ 8.01 (ddd, 4 H, J = 2, 8, 8 Hz, H$_c$), 7.90 (d, 4 H, J = 4 Hz, H$_a$), 7.88 (d, 4 H, J = 8 Hz, H$_d$), 7.57 (dd, 4 H, J = 5, 8 Hz, H$_b$), 7.29−7.11 (m, 3.5 H, toluene), 4.40 (m, 4 H, H$_f$), 3.98 (m, 4 H, H$_f$′). IR (KBr, cm^{-1}): 3074 w, 3020 w, pyridine C−H; 1602 s, 1571 m, py C═N; 1483 m, 1438 s, pyridine C═C; 1142 vs, 1112 vs, 1091 vs, ClO$_4$; 3287 w, 2924 w, 1483 m, 1014 m, 912 m, 762 s. 742 m, 636 m, 626 s. Anal. Calcd for C$_{27.5}$H$_{30}$CdCl$_2$N$_6$O$_8$: C, 43.70; H, 4.00; N, 11.12. Found: C, 42.26; H, 3.88; N, 10.72.

X-ray Crystallography. Selected crystallographic data are given in Table 1, selected bond distances in Table 2, and selected bond angles in Table 3. Thermal ellipsoid plots are shown in Figures 1, 2, and 3, with complete atom labeling in Figures S1, S2, and S3 of the Supporting Information. Data were collected at 21 °C on a Siemens P4S four-circle diffractometer using a graphite-monochromated Mo Kα X-radiation (λ = 0.710 73 Å) and the θ−2θ technique over a 2θ range of 3−55°. During data collection three standard reflections were measured after every 97 reflections. Both crystals turned black in the beam. The structures were solved by direct methods and Fourier difference maps using the SHELXTL-PLUS[12] package of software programs. Final refinements were done using SHELXL-93[13] minimizing

(8) (a) Granger, P. In *Transition Metal Nuclear Magnetic Resonance*; Pregosin, P. S., Ed.; Elsevier: New York, 1991; pp 306−346. (b) Santos, R. A.; Gruff, E. S.; Koch, S. A.; Harbison, G. S. *J. Am. Chem. Soc.* **1991**, *113*, 469.
(9) Bebout, D. C.; Ehmann, D. E.; Trinidad, J. C.; Crahan, K. K.; Kastner, M. E.; Parrish, D. A. *Inorg. Chem.* **1997**, *36*, 4257.
(10) Bebout, D. C.; DeLanoy, A. E.; Ehmann, D. E.; Kastner, M. E.; Parrish, D. A.; Butcher, R. J. *Inorg. Chem.* **1998**, *37*, 2952.
(11) (a) Wosley, W. C. *J. Chem. Educ.* **1973**, *50*, A335. (b) Raymond, K. N. *Chem. Eng. News* **1983**, *61* (49), 4.
(12) *SHELXTL-Plus*, Version 4.21/V; Siemens Analytical X-ray Instruments, Inc.: Madison, WI, 1990.
(13) Sheldrick, G. M. *Crystallographic Computing 6*; Flack, H. D., Parkanyi, L., Simon, K., Eds.; Oxford University Press: Oxford, 1993; p 111.

Table 1. Selected Crystallographic Data

	$[Cd(TMPA)_2](ClO_4)_2$·toluene (**1**)	$[Cd(BMPA)(NCCH_3)(OH_2)(OClO_3)]$-$[Cd(BMPA)_2](ClO_4)_3(CH_3CN)$ (**2**)
empirical formula	$C_{43}H_{44}N_8O_8Cl_2Cd$	$C_{40}H_{47}N_{11}O_{17}Cl_4Cd_2$
fw	984.16	1320.49
space group	triclinic, $P1$	triclinic, $P\bar{1}$
a, Å	9.629(2)	10.466(2)
b, Å	11.020(2)	16.653(3)
c, Å	11.641(2)	17.736(3)
α, deg	114.069(13)	62.479(9)
β, deg	97.492(13)	80.606(14)
γ, deg	91.034(14)	84.66(2)
V, Å^3	1114.7(3)	2699.0(9)
Z	1	2
d_{calc}, Mg/m^{-3}	1.466	1.625
μ, cm^{-1}	6.71	10.62
radiation (monochromatic)	Mo Kα ($\lambda = 0.710\ 73$ Å)	Mo Kα ($\lambda = 0.710\ 73$ Å)
T, °C	21	21
R1[a]	0.0519	0.0973
R2[b]	0.1222	0.2310

[a] $R1 = \sum||F_o| - |F_c||/\sum|F_o|$. [b] $R2 = [\sum[w(F_o^2 - F_c^2)^2]/\sum[w(F_o^2)^2]^{1/2}$.

Table 2. Selected Bond Distances (Å) in $[Cd(TMPA)_2](ClO_4)_2$· toluene (**1**) and $[Cd(BMPA)(NCCH_3)(OH_2)(OClO_3)]$-$[Cd(BMPA)_2](ClO_4)_3(CH_3CN)$ (**2**)

$[Cd(TMPA)_2](ClO_4)_2$· toluene (**1**)		$[Cd(BMPA)(NCCH_3)(OH_2)(OClO_3)]$-$[Cd(BMPA)_2](ClO_4)_3(CH_3CN)$ (**2**)	
Cd−N(1)	2.576(11)	Cd(1)−N	2.263(8)
Cd−N(2)	2.491(12)	Cd(1)−N(A)	2.321(8)
Cd−N(11)	2.529(13)	Cd(1)−N(1)	2.281(7)
Cd−N(12)	2.501(11)	Cd(1)−N(2)	2.285(7)
Cd−N(13)	2.610(13)	Cd(1)−O(1W)	2.313(7)
Cd−N(21)	2.520(12)	Cd(1)−O(11)	2.478(7)
Cd−N(22)	2.478(10)	Cd(2)−N(2A)	2.398(5)
Cd−N(23)	2.630(13)	Cd(2)−N(2B)	2.392(5)
		Cd(2)−N(21)	2.356(6)
		Cd(2)−N(22)	2.374(5)
		Cd(2)−N(23)	2.355(6)
		Cd(2)−N(24)	2.364(6)

$R2 = [\Sigma[w(F_o^2 - F_c^2)^2]/\Sigma[w(F_o^2)^2]]^{1/2}$, $R1 = \Sigma| |F_o| - |F_c| |/\Sigma|F_o|$, and $S = [\Sigma[w(F_o^2 - F_c^2)^2]/(n - p)]^{1/2}$. All non-hydrogen atoms were refined as anisotropic and the hydrogen atomic positions were fixed relative to the bonded carbons and the isotropic thermal parameters were fixed.

X-ray Diffraction of $[Cd(TMPA)_2](ClO_4)_2$·toluene (1). A crystal measuring 0.3 × 0.4 × 0.3 mm was glued on the end of glass fiber. No decay of the intensity of the standard was observed and no absorption correction was performed on these data. ψ scans showed significant variation (23%) and a semiempirical absorption correction was applied to the data. The final data-to-parameter ratio was 9:1.

X-ray Diffraction of $[Cd(BMPA)(NCCH_3)(OH_2)(OClO_3)][Cd(BMPA)_2](ClO_4)_3$·$(CH_3CN)$ (2). The crystal measured 0.36 × 0.99 × 0.40 mm. The intensity of the standards decreased about 12% during data collection and all data was scaled based on the standards. ψ curves showed significant variation (29%) and a semiempirical absorption correction was applied to the data. The final data-to-parameter ratio was 15:1.

NMR Measurements. All solutions for NMR analysis were prepared by adding stock solutions of TMPA in acetonitrile-d_3 to a solution of mercuric perchlorate or mercuric chloride in acetonitrile-d_3 using calibrated autopipets. NMR spectra were recorded in 5-mm-o.d. NMR tubes on a General Electric QE-300 operating in the pulse Fourier transform mode. The sample temperature was maintained by blowing chilled air over the NMR tube in the probe. The variable temperature unit was calibrated with methanol as previously described.[14] Chemical shifts were measured relative to internal solvent but are reported relative to tetramethylsilane.

(14) Raiford, D. S.; Fisk, C. L.; Becker, E. D. *Anal. Chem.* **1979**, *51*, 2050.

Table 3. Selected Bond Angles (deg) in $[Cd(TMPA)_2](ClO_4)_2$· toluene (**1**) and $[Cd(BMPA)(NCCH_3)(OH_2)(OClO_3)]$-$[Cd(BMPA)_2](ClO_4)_3(CH_3CN)$ (**2**)

$[Cd(TMPA)_2](ClO_4)_2$· toluene (**1**)		$[Cd(BMPA)(NCCH_3)(OH_2)(OClO_3)]$-$[Cd(BMPA)_2](ClO_4)_3(CH_3CN)$ (**2**)	
N(1)−Cd−N(2)	178.6(5)	N−Cd(1)−N(A)	173.5(5)
N(1)−Cd−N(11)	66.2(4)	N−Cd(1)−N(1)	101.5(3)
N(1)−Cd−N(12)	67.1(3)	N−Cd(1)−N(2)	111.6(3)
N(1)−Cd−N(13)	64.1(4)	N−Cd(1)−O(1W)	81.6(3)
N(2)−Cd−N(21)	67.6(4)	N−Cd(1)−O(11)	88.2(3)
N(2)−Cd−N(22)	66.2(4)	N(A)−Cd(1)−N(1)	72.9(3)
N(2)−Cd−N(23)	64.9(4)	N(A)−Cd(1)−N(2)	73.7(3)
N(1)−Cd−N(21)	113.6(4)	N(A)−Cd(1)−O(1W)	102.0(4)
N(1)−Cd−N(22)	112.7(4)	N(A)−Cd(1)−O(11)	87.8(4)
N(1)−Cd−N(23)	115.0(4)	N(1)−Cd(1)−N(2)	146.5(3)
N(2)−Cd−N(11)	112.6(4)	N(1)−Cd(1)−O(1W)	94.7(3)
N(2)−Cd−N(12)	114.0(3)	N(1)−Cd(1)−O(11)	84.6(3)
N(2)−Cd−N(13)	116.0(4)	N(2)−Cd(1)−O(1W)	94.9(3)
N(11)−Cd−N(12)	103.3(4)	N(2)−Cd(1)−O(11)	91.3(2)
N(11)−Cd−N(13)	105.9(4)	O(1W)−Cd(1)−O(11)	169.5(3)
N(11)−Cd−N(21)	179.4(6)	N(2A)−Cd(2)−N(2B)	142.2(2)
N(11)−Cd−N(22)	75.7(4)	N(2A)−Cd(2)−N(21)	71.7(2)
N(11)−Cd−N(23)	73.6(4)	N(2A)−Cd(2)−N(22)	71.3(2)
N(12)−Cd−N(13)	103.9(4)	N(2A)−Cd(2)−N(23)	98.3(2)
N(12)−Cd−N(21)	76.2(4)	N(2A)−Cd(2)−N(24)	141.8(2)
N(12)−Cd−N(22)	178.9(5)	N(2B)−Cd(2)−N(21)	142.1(2)
N(12)−Cd−N(23)	75.6(4)	N(2B)−Cd(2)−N(22)	96.7(2)
N(13)−Cd−N(21)	74.4(4)	N(2B)−Cd(2)−N(23)	71.7(2)
N(13)−Cd−N(22)	76.9(4)	N(2B)−Cd(2)−N(24)	71.9(2)
N(13)−Cd−N(23)	179.1(6)	N(21)−Cd(2)−N(22)	114.7(2)
N(21)−Cd−N(22)	104.8(4)	N(21)−Cd(2)−N(23)	90.4(2)
N(21)−Cd−N(23)	106.2(4)	N(21)−Cd(2)−N(24)	85.6(2)
N(22)−Cd−N(23)	103.6(4)	N(22)−Cd(2)−N(23)	146.5(2)
		N(22)−Cd(2)−N(24)	92.2(2)
		N(23)−Cd(2)−N(24)	112.5(2)

Results

Crystal Structure of X-ray Diffraction of $[Cd(TMPA)_2](ClO_4)_2$·toluene (1). This complex appears to be the first example of a structurally characterized eight-coordinate Cd(II) complex in which all the donor nitrogens are part of chelating organic ligands. The only other structurally characterized TMPA complexes of this type are $[Mn(TMPA)_2](ClO_4)_2$[15] and $[Hg(TMPA)_2](ClO_4)_2$ (**6**)[9] although a similar complex of $NaClO_4$[16]

(15) Gultneh, Y.; Farooq, A.; Karlin, K. D.; Liu, S.; Zubieta, J. *Inorg. Chim. Acta* **1993**, *211*, 171.

(16) Toftlund, H.; Ishiguro, S. *Inorg. Chem.* **1989**, *28*, 2236.

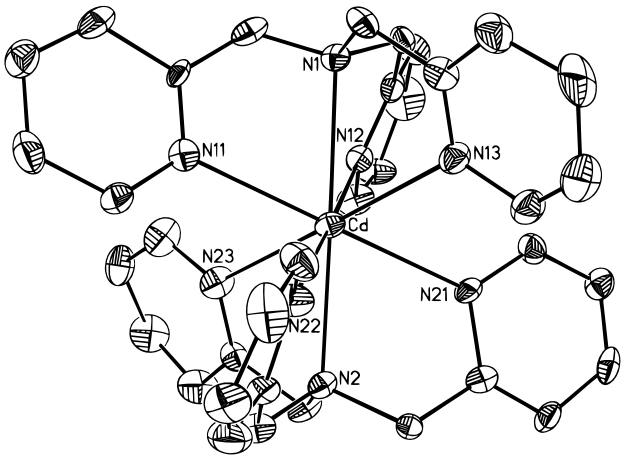

Figure 1. Thermal ellipsoid plot of the $[Cd(TMPA)_2]^{2+}$ cation of **1**. Ellipsoids are at 20% probability. Hydrogens are omitted for clarity.

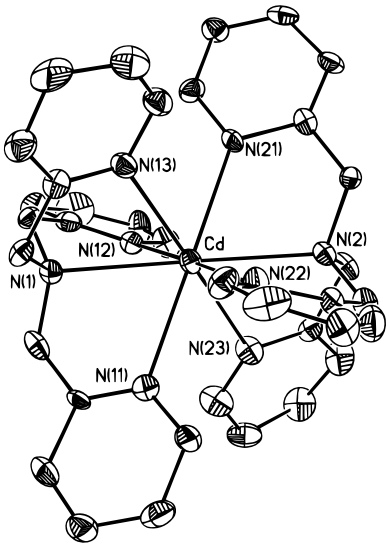

Figure 2. Thermal ellipsoid plot of the $[Cd(BMPA)_2]^{2+}$ dication of **2**. Ellipsoids are at 20% probability. Hydrogens are omitted for clarity.

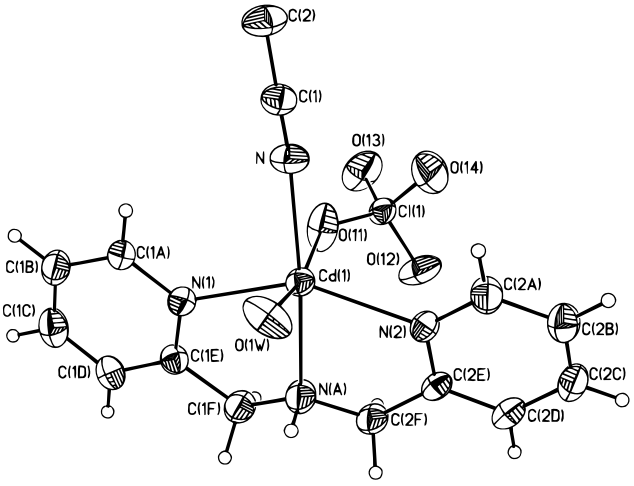

Figure 3. Thermal ellipsoid plot of the $[Cd(BMPA)(NCCH_3)(OH_2)(OClO_3)]^+$ monocation of **2**. Ellipsoids are at 20% probability. Acetonitrile hydrogens are omitted for clarity.

has been proposed. Complex **6** possesses an inversion center which is not present in the Cd(II) or Mn(II) complexes, but their metal coordination environments are similar in all other aspects. The metal−nitrogen bond lengths in the Cd(II) complex are less than 2% shorter than those in the Hg(II) complex and less than 3% longer than those in the Mn(II) complex. The average metal−N_{amine} are nearly the same as the average metal−$N_{pyridyl}$ distances in the three complexes (Δ = 0.01, 0.02, and 0.03 Å for Cd(II), Hg(II), and Mn(II), respectively). The Cd(II) complex intraligand $N_{amine}-N_{pyridyl}$ distances of 2.77(3) Å, interligand $N_{amine}-N_{amine}$ distances of 3.12(5) Å, and N−N−N angles ranging from 81 to 96° are also comparable to the same measurements for the other complexes.

Crystal Structure of $[Cd(BMPA)(NCCH_3)(OH_2)(OClO_3)]\cdot[Cd(BMPA)_2](ClO_4)_3\cdot(CH_3CN)$ (2). Both cations of **2** possess six-coordinate Cd(II). The complex $[Cd(BMPA)_2](ClO_4)_2$ (**7**) with a crystallographic 2-fold axis has previously been isolated independently,[17] and we prepared $[Cd(BMPA)_2](ClO_4)_2\cdot$0.5toluene (**5**) for NMR characterization in this work. In **2**, the 1:2 metal-to-ligand ratio cation (**2a**) has only molecular C_2 symmetry but is otherwise similar to **7** with the ligands oriented facially in a pseudo-trigonal prismatic geometry. We recently reported that **7** was similar in structure to $[Hg(BMPA)_2](ClO_4)_2\cdot$0.5toluene (**8**).[10] The average Cd−N_{amine} bond length of 2.362(8) Å and average Cd−$N_{pyridyl}$ bond length of 2.395(5) Å in **2a** are less than 2% shorter than in **8**. The average **2a** intraligand N_{amine}−Cd−$N_{pyridyl}$ and $N_{pyridyl}$−Cd−$N_{pyridyl}$ bond angles of 71.7(2)° and 113.6(11)°, respectively, are also similar to those in **8** indicating the ligands are in a similar conformation. The largest differences between **2a** and **8** appears to be the relative orientation of the two ligands around the metal as indicated by interligand N_{amine}−Cd−N_{amine} bond angles of 142.2(2)° and 153.1(2)°, respectively.

A variety of metal complexes of type $[M(BMPA)_2]$ with noncoordinating counterions have been isolated. Some of these (M = Cd(II), Mn(II), Zn(II),[17] and Hg(II)[10]) possess either crystallographic or molecular C_2 symmetry with the ligands oriented facially in a pseudo-trigonal prismatic geometry as in **2a**. In contrast, an Fe(II) complex with crystallographic C_2 symmetry has intraligand $N_{pyridyl}$−Cd−$N_{pyridyl}$ bond angles ranging between 82° and 85° involving *facial* BMPA coordination and *cis*-N_{amines}.[18] Complexes with C_i symmetry (M = Cu(II),[19] Zn(II)[17]) are also known which can be described as pseudo-octahedral involving facial BMPA coordination with *trans*-N_{amines}. In most of these $[M(BMPA)_2]$ complexes, the M−N_{amine} and M−$N_{pyridyl}$ bond lengths are similar. As a result, rearrangment between various trigonal prismatic and octahedral structures is anticipated to occur readily by rotation about pseudo-C_3.[10,20] The small structural differences between the two structurally characterized Cd(II) structures emphasize the malleability of the coordination sphere.

The 1:1 metal-to-ligand ratio cation of **2** (**2b**) is structurally similar to the recently reported complex $[Hg(BMPA)(NCCH_3)](ClO_4)_2$ (**9**).[10] In **9**, the Hg−N_{amine} distance was approximately 0.18 Å longer than the other three Hg−N distances which averaged 2.23(3) Å. Similarly, in **2b** the Cd−N_{amine} distance is longest, but only by approximately 0.045 Å compared to the 2.276(9) Å average of the other three Cd−N distances. The overall average of the metal-nitrogen bond lengths is 0.02 Å longer in **2b** than in **9**, possibly due to stronger metal−oxygen bonds. The axial Cd−O bond lengths in **2b** are 2.313 and 2.478

(17) Glerup, J.; Goodson, P. A.; Hodgson, D. J.; Michelsen, K.; Nielson, K. M.; Weihe, H. *Inorg. Chem.* **1992**, *31*, 4611.
(18) Butcher, R. J.; Addison, A. W. *Inorg. Chim. Acta* **1989**, *158*, 211.
(19) Palaniandavar, M.; Butcher, R. J.; Addison, A. W. *Inorg. Chem.* **1996**, *35*, 467.
(20) (a) Rodger, A.; Johnson, B. F. G. *Inorg. Chem.* **1988**, *27*, 3061. (b) Bailar, J. C., Jr. *J. Inorg. Nucl. Chem.* **1958**, *8*, 165. (c) Ray, P. C.; Dutt, N. K. *Indian Chem. Soc.* **1943**, *20*, 81.

Å for water and perchlorate, respectively. In **9**, two axial perchlorates form close associations with Hg−O distances of 2.707(7) and 2.90(2) Å. The $N_{pyridine}$−metal−$N_{pyridine}$ bond angle of 146.5(3)° in **2b** is 11.5° larger than in **9** but otherwise BMPA appears to have a very similar geometry.

Investigation of TMPA Coordination of Cd(II) in the Solution State. Acetonitrile-d_3 solutions containing nominal molar ratios of TMPA and $Cd(ClO_4)_2$ were examined by proton NMR with total [Cd(II)] = 2 mM. Selected proton NMR spectra are shown in Figure 4. The only significant difference between the proton NMR of **1** (Figure 4a) and a sample prepared from corresponding stoichiometric amounts of metal and ligand were the toluene resonances. The chemical shifts of selected ^1H resonances as a function of [Cd(II)]/[TMPA] at 20 °C are shown in Figure 5 superimposed on the previously reported data for Hg(II).[9] The chemical shift trends for all ligand protons are shown in Figure S4.

In general, TMPA proton chemical shifts in the presence of various mole ratios of Cd(II) were only slightly upfield of the values with Hg(II). The similarity in proton chemical shift trends as a function of [metal]/[TMPA] for Cd(II) and Hg(II) suggests that the solution equilibria are very similar in the two systems. With both metals, there is slow exchange between free ligand and an apparent 1:2 metal-to-ligand complex at [metal]/[TMPA] < 0.5. Between 0.5 and 1.0 equiv metal, there is a rapid change in the chemical shifts of most protons, followed by essentially constant chemical shifts above [metal]/[TMPA] = 1.0. We have previously analyzed the Hg(II) system in the context of the following equilibria:

$$M^{2+} + TMPA \rightleftharpoons [M(TMPA)]^{2+} \quad (1)$$

$$[M(TMPA)]^{2+} + TMPA \rightleftharpoons [M(TMPA)_2]^{2+} \quad (2)$$

$$[M(TMPA)_2]^{2+} + [M(TMPA)]^{2+} \rightleftharpoons [M_2(TMPA)_3]^{4+} \quad (3)$$

$$[M_2(TMPA)_3]^{4+} + [M(TMPA)]^{2+} \rightleftharpoons [M_3(TMPA)_4]^{6+} \quad (4)$$

$$[M_2(TMPA)_3]^{4+} + M^{2+} \rightleftharpoons 3\,[M(TMPA)]^{2+} \quad (5)$$

The discontinuity at [metal]/[BMPA] = 0.5 suggests the net equilibrium constant for formation of $[M(TMPA)_2]^{2+}$ must be much larger than that for formation of $[M(TMPA)]^{2+}$ for both metals. This is consistent with previously reported formation constants

$$\beta_2 = [M(L)_2]/[M][L]^2 \quad (6)$$

and

$$\beta_1 = [M(L)]/[M][L] \quad (7)$$

for the TMPA complexes of metal nitrates at 25 °C in aqueous solution indicating β_2 was 4 and 7 orders of magnitude larger for Cd(II) and Hg(II), respectively.[21] Furthermore, a smaller difference between the formation constants of the Cd(II) complexes is suggested by detectable resonances for the 1:2 metal:ligand complexes at higher [metal]/[TMPA] than observed with Hg(II).

If only 1:2 and 1:1 metal-to-ligand species were present in the region between 0.5 < [metal]/[TMPA] < 1.0, the exchange-averaged chemical shift, δ_{obs}, would be expected to change approximately linearly according to expression 8

$$\delta_{obs} = P_{1:1}\delta_{1:1} + (1 - P_{1:1})\delta_{1:2} \quad (8)$$

in which $\delta_{1:1}$ and $\delta_{1:2}$ are the chemical shifts and $P_{1:1}$ and $P_{1:2}$ [=0.5(1 − $P_{1:1}$)] are the mole fractions of 1:1 and the 1:2 metal-to-ligand complexes, respectively. Significant deviations from linearity in this region with Hg(II), as well as trends in

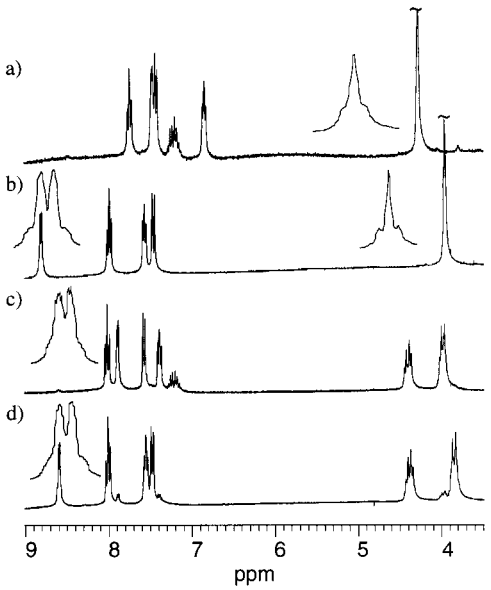

Figure 4. Selected proton NMR spectra in CD_3CN with total [Cd(II)] = 2 mM at 20 °C. (a) $[Cd(TMPA)_2](ClO_4)_2$·toluene (**1**). Expanded inset for H_f shows slight exchange broadening. (b) [Cd]/[TMPA] = 1.375. Expanded insets are shown for H_a and H_f. (c) $[Cd(BMPA)_2](ClO_4)_2$·0.5toluene (**5**). Expanded inset shown for H_a. (d) [Cd]/[BMPA] = 1.1. Minor peaks at 7.90, 7.38, and 3.98 ppm are associated with the cations of **5**. Expanded inset shown for H_a.

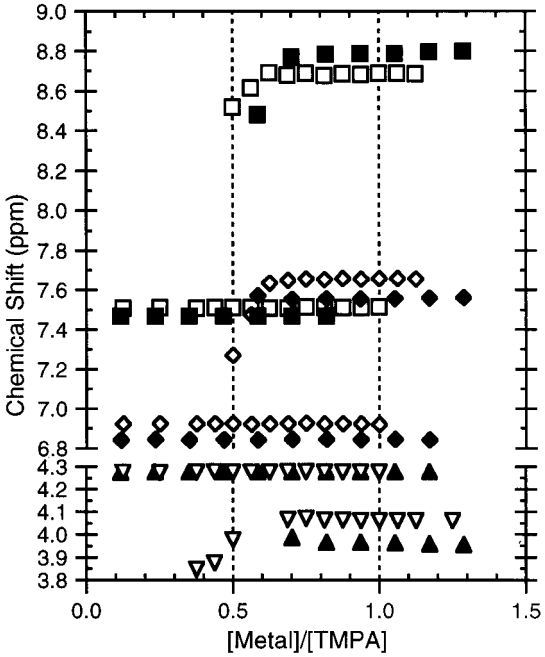

Figure 5. Chemical shifts of selected protons of TMPA in the presence of $Cd(ClO_4)_2$ (filled symbols) or $Hg(ClO_4)_2$ (open symbols) as a function of the nominal metal-to-ligand ratio in CD_3CN at 20 °C. Total metal concentration was 2 mM. Chemical shifts associated with a second ligand environment consisting primarily of free ligand in the region below [metal]/[TMPA] = 0.5 are omitted for clarity. H_a = square; H_b = diamond; H_f = triangle.

(21) Anderegg, G.; Hubmann, E.; Podder, N. G.; Wenk, F. *Helv. Chim. Acta* **1977**, *60*, 123.

Table 4. Coupling Constants (J), Reduced Coupling Constants (K), and Estimated Relativistically Adjusted Reduced Coupling Constants (K_{RA}) for Hg(II) and Cd(II) Complexes of TMPA and BMPA

		M = Hg[a,b]			M = Cd[b]		
complex	proton	J (Hz)	K[c]	K_{RA}[c,d]	J (Hz)	K[c,e]	K_{RA}[c,d]
$[M(TMPA)_2]^{2+}$	H_f	46	215	67	8	31	21
$[M(TMPA)]^{2+}$	H_a	40	189	60	9	35	24
	H_d	20	93	30			
	H_f	36	168	54	8	31	21
$[M(BMPA)_2]^{2+}$	H_a	20[c]	93	30	6	23	16
	H_f	69[c]	322	103			
	H_f'	72[c]	336	107			
$[M(BMPA)]^{2+}$	H_a	80	373	119	9	35	24
	H_d	24	112	36			
	H_f	80	373	119			
	H_f'	42	196	63			

[a] Coupling constants for Hg(II) complexes are from refs 9 (TMPA) and 10 (BMPA). [b] Determined at 20 °C (except $[Hg(BMPA)_2]^{2+}$ which was determined at −40 °C) in acetonitrile-d_3 with a complex concentration of 2 mM with perchlorate counterions. [c] K and K_{RA} are in SI units of N A^{-2} m^{-3} and multiplied by a factor of 10^{18}. [d] The K_{RA} were estimated using multiplicative one-bond coupling factors of 1.45 and 3.13 for Cd (ref 27) and Hg (ref 28), respectively. [e] A weighted average has been used for the magnetogyric ratio of cadmium since separate satellites were not resolvable with the magnitude of the coupling observed here.

temperature and concentration dependence, led to the proposed involvement of multinuclear species in equilibria 3 and 4.

The prevalence of rapid exchange in the solution-state coordination chemistry of Cd(II) and Hg(II) makes detection of heteronuclear coupling between ligand protons and the NMR active isotopes of both these metals very notable. At [metal]/[TMPA] < 0.5, the observed couplings are assigned to $[M(TMPA)_2]^{2+}$, the cations structurally characterized in **1** and **6**. At [metal]/[TMPA] > 1.0, the cation $[M(TMPA)]^{2+}$, or possibly its solvate $[M(TMPA)(NCCH_3)]^{2+}$, is assigned to the couplings associated with the major peaks. The magnitudes of the observed couplings are provided in Table 4. The similar magnetogyric ratios of ^{113}Cd and ^{111}Cd, −5.9330 and −5.6720 × 10^{-7} rad/T s, respectively, lead to satellite overlap at the small splittings observed here. The coupling satellites accounted for approximately 17% and 25% of the area of associated resonances as expected on the basis of the natural abundances of ^{199}Hg and $^{111/113}$Cd, respectively. The significance of the larger and more extensive couplings in the Hg(II) system is amplified in the Discussion.

Investigation of BMPA Coordination of Cd(II) in the Solution State. Acetonitrile-d_3 solutions containing nominal molar ratios of BMPA and $Cd(ClO_4)_2$ were examined by proton NMR with total [Cd(II)] = 2 mM. Selected proton NMR spectra are shown in Figure 4. The only significant difference between the proton NMR of **5** (Figure 4c) and a sample prepared from corresponding stoichiometric amounts of metal and ligand were the toluene resonances. The chemical shifts of the selected ^{1}H resonances as a function of [Cd(II)]/[BMPA] at 20 °C are shown in Figure 6 superimposed on the previously reported data for Hg(II).[10] The chemical shift trends for all ligand protons are shown in Figure S5.

As with TMPA, the BMPA proton chemical shifts in the presence of various mole ratios of Cd(II) were generally only slightly upfield of the values with comparable mole ratios of Hg(II). The similar trends in chemical shifts as a function of [metal]/[BMPA] suggests that the solution equilibria are comparable in the two systems. We have previously analyzed the

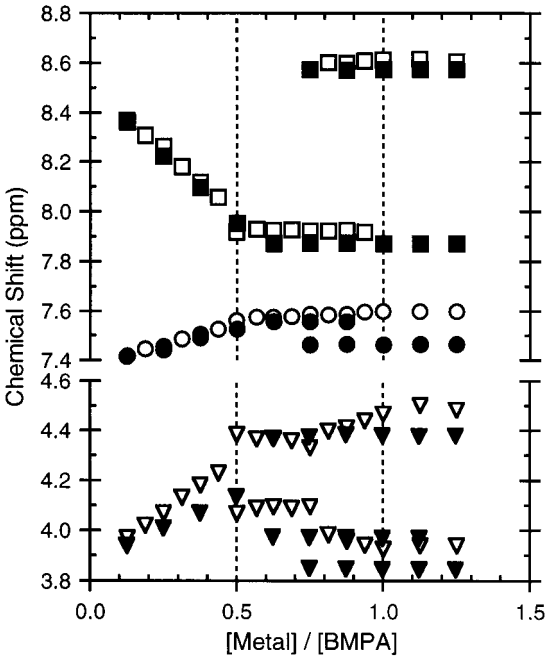

Figure 6. Chemical shifts of selected protons of BMPA in the presence of $Cd(ClO_4)_2$ (filled symbols) or $Hg(ClO_4)_2$ (open symbols) as a function of the nominal metal-to-ligand ratio in CD_3CN at 20 °C. Total metal concentration was 2 mM. H_a = square; H_d = circle; H_f = triangle.

Hg(II) system in the context of the following equilibria:

$$M^{2+} + BMPA \rightleftharpoons [M(BMPA)]^{2+} \quad (9)$$

$$[M(BMPA)]^{2+} + BMPA \rightleftharpoons [M(BMPA)_2]^{2+} \quad (10)$$

$$[M(BMPA)_2]^{2+} + BMPA \rightleftharpoons [M(BMPA)_3]^{2+} \quad (11)$$

$$[M(BMPA)_2]^{2+} + M^{2+} \rightleftharpoons 2\,[M(BMPA)]^{2+} \quad (12)$$

The net equilibrium constant for formation of $[M(BMPA)_2]^{2+}$ must be much larger than that for formation of $[M(BMPA)]^{2+}$ for both metals to explain the discontinuity at [metal]/[BMPA] = 0.5. Previously reported formation constants for the $Cd(NO_3)_2$ complexes of BMPA at 25 °C in aqueous solution suggest β_2 is approximately 5 orders of magnitude greater than β_1 in the system examined in this work.[21] Unfortunately, only β_2 was reported for $Hg(NO_3)_2$.

With low total metal concentrations, there is rapid exchange between free ligand and the 1:2 metal-to-ligand complex at [metal]/[BMPA] < 0.5. Under these conditions, the chemical shifts of the exchange-averaged resonances changed approximately linearly with [metal]/[BMPA] as predicted by an expression similar to 8 but with terms for free ligand and the 1:2 metal-to-ligand complex. At metal concentrations in excess of 100 mM, significant deviations from linearity for H_a and H_d in this region with Hg(II) suggested equilibrium 11 roughly described the rapid exchange between free and bound ligand. Similar deviations were not observed with 100 mM Cd(II) solutions (data not shown) and no further attempt was made to characterize this exchange process.

With both metals, the chemical shift trends change for all protons at [metal]/[BMPA] = 0.5. Most notable is the appearance of two separate chemical shift environments for the H_f. A second set of proton resonances associated with a 1:1 metal-to-ligand complex begins to grow in at [metal]/[BMPA] ≈ 0.75. As discussed previously for the Hg(II) system,[10] the equivalence

of the six M−N bond lengths in **2b** suggests a solution structure involving equilibration between two achiral *facial* octahedral species and three sets of trigonal prismatic enantiomeric pairs. Since there are two environments for H_f, a *meridional* octahedral isomer which would permit inversion at the amine nitrogen is excluded from the equilibration on the NMR time scale. The slow exchange on the NMR time scale for H_d and the upfield H_f resonance in the Cd(II) system is one of the most significant chemical shift differences with the Hg(II) system. Also notable is the continued presence of resonances for **2a** with [Cd(II)]/[BMPA] between 1.0 and 1.5. In the Hg(II) system, the 1:2 metal-to-ligand complex was not detectable at [Hg(II)]/[BMPA] > 1.0, consistent with the relative difference between β_2 and β_1 being larger for Hg(II) than Cd(II).

In contrast to the very similar trends in chemical shifts as a function of [metal]/[BMPA] indicating comparable solution equilibria, the detectable coupling constants between the protons of BMPA and $^{111/113}$Cd were considerably smaller in magnitude than those to ^{199}Hg (Table 4). Furthermore, although ^{199}Hg coupled to H_a and H_f in both complexes, $^{111/113}$Cd was only observed to couple with H_a. Interestingly, slow-exchange conditions were established for $[Cd(BMPA)_2]^{2+}$ at 20 °C but significant cooling and a slight excess of metal was required for resolution of coupling satellites for the related Hg(II) complex. This is most likely related to the higher ionic radius of Hg(II) facilitating associative exchange processes. It is also important to note that the coupling constant comparison of the two $[M(BMPA)]^{2+}$ cations requires the assumption that axial coordination is comparable for the two metals in the solution state since coordination number affects *s*-electron density at the nucleus (vide infra).

Discussion

Numerous investigators have prepared Cd(II) and Hg(II) coordination compounds of identical ligand systems. However, only rarely have satellites due to proton coupling to the metal nuclei with spin $I = {}^1/_2$ been reported in the solution-state.[22] As a result, Cd(II) and Hg(II) solution state chemical shifts have typically been measured by direct means with concentrated, isotopically enriched samples. Coupling to abundant, sensitive nuclei like protons is instrumental to measuring metal chemical shifts by the coherence transfer techniques being increasingly applied to Cd(II) and Hg(II) substituted proteins. Identification of slow-exchange NMR conditions for several essentially isostructural Cd(II) and Hg(II) nitrogen coordination compounds provides an exceptional opportunity to investigate contributions to the magnitude of metal-proton coupling constants. In four of the five studies that we have been able to identify, coupling with ^{199}Hg was larger and usually more extensive than with $^{111/113}$Cd to the protons of nitrogen-coordinated ligands.[22a−d] However, crystallographic and extensive solution-state NMR comparisons of the Hg(II) and Cd(II) complexes was only provided in one instance.[22a] The one study reporting $J(^1H^{111/113}Cd) > J(^1H^{199}Hg)$ involved a potentially hexadentate macrocycle and only the structure of the Hg(II) complex of this macrocycle was reported.[22e] The difference between the ionic radii of Hg(II) and Cd(II) is expected to produce significant differences in the geometry of coordinated macrocycles which complicate direct comparison of coupling. A number of metalloproteins have been investigated by NMR following substitution with Cd(II)[4,23] or Hg(II)[3,4,5] and verification of the preservation of the native metal coordination sphere. Only in the case of rubredoxin, in which all the metal chelating groups are sulfur-based, have coupling constants been reported for both metals and $J(^1H^{199}Hg)$ was approximately 2-fold stronger than $J(^1H^{111/113}Cd)$.[4]

The X-ray crystallographic and acetonitrile solution-state chemical shift data presented here provide compelling evidence for the structural similarity of the TMPA and BMPA complexes of the perchlorate salts of Hg(II) and Cd(II). Although correlations between solid-state structures and solution-state NMR properties must always be made carefully,[24] the extensive heteronuclear couplings between ^{199}Hg and the protons of these two ligands were very instrumental in highlighting the relationships between the structures in the two states. In contrast, the heteronuclear couplings in the isovalent $^{111/113}$Cd system are much more limited and substantially smaller in magnitude. Significantly, this set of structurally comparable complexes includes a number of different coordination numbers and geometries suggesting the coupling constant trends are general, at least for ligands coordinated through nitrogen.

The paucity of coupling constant data for coordination compounds of Hg(II) and Cd(II) stems largely from rapid metal−ligand exchange rates compared to the NMR time scale. The low coordination geometry preferences and ability to adopt up to three different coordination numbers with one ligand type contributes to the prevalence of rapid exchange with these d^{10} metal ions. Hg(II) typically has a higher affinity for nitrogen-based ligands than any other divalent metal ion, but its large ionic radius readily accommodates associative exchange processes. A common, though not sufficient, feature of the nitrogen-based ligand systems in which coupling has been detected is a minimum of three donor atoms.[22] Optimization of concentration, solvent, temperature and metal-to-ligand ratio are all necessary to favor detection of coupling between the nuclei of metals and ligands.[9,10]

There are many contributing factors to the magnitudes of indirect nuclear spin−spin coupling constants. The magnitudes of three-bond coupling constants are commonly related to molecular structure through a Karplus-type relationship of the general form

$$^3J_{XY} = A\cos 2\phi + B\cos\phi + C \qquad (13)$$

where ϕ is the dihedral angle and *A*, *B*, and *C* are empirical constants.[25] Based on data derived almost exclusively from alkylmercurials, $^3J(^1H^{199}Hg)$ is associated with a Karplus-type of dependency on dihedral angles.[26] Recently, coordination compounds of Hg(II) in slow exchange on the NMR time scale in the solution-state have been characterized which also suggest a Karplus-type of relationship for $^3J(^1H^{199}Hg)$.[9,10] However, the Karplus equation must be used very carefully because other

(22) (a) Schlager, O.; Wieghardt, K.; Grondey, H.; Rufi'nska, A.; Nuber, B. *Inorg. Chem.* **1995**, *34*, 6440. (b) McWhinnie, W. R.; Monsef-Mirzai, Z.; Perry, M. C.; Shaikh, N.; Hamor, T. A. *Polyhedron* **1993**, *12*, 1193. (c) Nivorozhkin, A. L.; Sukholenko, E. V.; Nivorozhkin, L. E.; Borisenko, N. I.; Minkin, V. I. *Polyhedron* **1989**, *8*, 569. (d) McCrindle, R.; Ferguson, G.; McAlees, A. J.; Parvez, M.; Ruhl, B. L.; Stephenson, D. K.; Wieckowski, T. *J. Chem. Soc., Dalton Trans.* **1986**, 2351. (e) Bashall, A.; McPartlin, M.; Murphy, B. P.; Powell, H. R.; Waikar, S. *J. Chem. Soc., Dalton Trans.* **1994**, 1383.

(23) (a) Pan, T.; Coleman, J. E. *Proc. Natl. Acad. Sci. U.S.A.* **1990**, *87*, 2077. (b) Otvos, J. D.; Engeseth, H. R.; Wehrli *J. Magn. Reson.* **1985**, *61*, 579. (c) Frey, M. H. Wagner, G.; Vašák, M.; Sørensen, O. W.; Neuhaus, D.; Wörgötter, E.; Kägi, J. H. R.; Ernst, R. R.; Wüthrich, K. *J. Am. Chem. Soc.* **1985**, *107*, 6847. (d) Live, D. H.; Kojiro, C. L.; Cowburn, D.; Markley *J. Am. Chem. Soc.* **1985**, *107*, 3043.

(24) Davies, J. A.; Dutremez, S. *Coord. Chem. Rev.* **1992**, *114*, 201.

(25) Mavel, G. *Annu. Rep. NMR Spectrosc.* **1973**, *5B*, 1.

(26) (a) Wrackmeyer, B.; Contreres, R. *Annu. Rep. NMR Spectrosc.* **1992**, *24*, 267. (b) Granger, P. In *Transition Metal Nuclear Magnetic Resonance*; Pregosin, P. S., Ed.; Elsevier: New York, 1991; p 306.

factors such as the electronegativity of substituents, hybridization, bond angles, and bond lengths also affect vicinal coupling.

Isolation of essentially isostructural Cd(II) and Hg(II) complexes provides on opportunity to investigate nuclear contributions to coupling constants in the absence of these other factors. Spin−spin couplings involving hydrogen are dominated by Fermi contact interaction which is related to the s-electron density at the nucleus.[27] The larger coupling constants for each of the Hg(II) complexes compared to the Cd(II) complexes is consistent with the prevalence of Fermi contact interaction. For evaluation of periodic trends, it is convenient to factor out the magnetogyric ratios of the coupled nuclei according to expression 13

$$J_{AB} = h\gamma_A\gamma_B K_{AB}/4\pi^2 \qquad (14)$$

where K_{AB} is defined as a reduced coupling constant. Reduced coupling constants have been provided in Table 4. Note that $|\gamma_{Cd}| > |\gamma_{Hg}|$ for both $I = {}^1/_2$ isotopes of cadmium, so this difference in nuclear properties actually enhances $^{111/113}$Cd spin−spin coupling constants.

For heavier elements, it is also important to consider relativistic effects on reduced coupling constants.Reduced coupling constants can also be adjusted for relativistic effects. Unfortunately, we have been unable to identify a relativistic treatment of longer-range coupling. Multiplicative relativistic adjustment factors of approximately 1.45[28] and 3.13[29] have been calculated for one-bond coupling with Cd(II) and Hg(II), respectively. In Table 4, estimated relativistic adjustments to the reduced coupling constants for each of the Cd(II) compounds discussed here and the isovalent Hg(II) compounds have been made using the one-bond coupling factors. Since relativistic effects fall off sharply with distance, the estimated K_{RA} represent minimum expected values yet differences ranging from a factor of 2 to 5 remain. These may primarily reflect the differences in s-electron density between the central atoms. In addition, long-range contributions may be more prevalent with ^{199}Hg. In alkylmercurials, coupling has been observed between ^{199}Hg and nuclei up to seven bonds away. Although there is no standard theory to explain these long range couplings, it is generally accepted that coupling constants are additive which can lead to significant enhancements if contributions are of the same sign.

Conclusion

While ^{113}Cd NMR has been used extensively over the last three decades as a structural metallobioprobe, development of alternative methods based on ^{199}Hg NMR have been largely neglected until very recently. Reservations to the development of ^{199}Hg NMR methods may have included the notoriously rapid metal exchange rates of simple Hg(II) complexes, speculation that ^{199}Hg spectra would have excessive line widths due to the large chemical shift anistropy associated with this nucleus, or the general impression that ^{199}Hg NMR offered no advantages over ^{113}Cd NMR. We have recently demonstrated that slow-exchange conditions on the NMR time scale can be identified for Hg(II) complexes of ligand systems designed to model the steric and electronic features of protein metal binding sites.[9,10,30] The handful of Hg(II)-substituted proteins which have been characterized by ^{199}Hg NMR have had reasonable line widths even in highly anisotropic three-coordinate binding sites.[3−6] The isostructural compounds compared here could be used to extend the available literature on the influence of geometry on the chemical shift anisotropy of Cd(II)[8,31] and Hg(II)[8,32] coordination compounds. Recently the potential of the shorter relaxation times and greater chemical shift dispersion of ^{199}Hg have been recognized.[3] In combination with a tendency to exhibit larger heteronuclear coupling constants with ^{1}H, at least with nitrogen based ligands, ^{199}Hg NMR methods appear to have some significant advantages as structural metallobioprobes over ^{113}Cd NMR methods. While additional comparisons with more diverse ligand geometries and donor atom compositions are necessary to more fully assess the relative advantages of these complementary NMR techniques, the prevalence of hisitidine and lysine in protein metal binding sites provides a strong incentive for further development of ^{199}Hg NMR methods.

Acknowledgment. This research was supported by the donors of the Petroleum Research Fund, administered by the American Chemical Society and by a Bristol-Meyers Squibb Company award of Research Corporation. R.J.B. acknowledges the DoD-ONR instrumentation program for funds to upgrade the diffractometer and the NIH-MBRS program for funds to maintain the diffractometer.

Supporting Information Available: Figures S1−S5, showing thermal ellipsoid plots and additional NMR data, and two X-ray crystallographic files, in CIF format, are available free of charge via the Internet at http://pubs.acs.org.

IC980825Y

(27) Jameson, C. J. In *Multinuclear NMR*; Jameson, C. J., Ed.; Plenum: New York, 1987; p 89.
(28) Jokissaari, P.; Räisänen, K.; Lajunen, L.; Passoja, A.; Pyykkö, P. *J. Magn. Reson.* **1978**, *31*, 121.
(29) Jokissaari, P.; Räisänen, K.; Kuonanoja, J.; Pyykkö, P.; Lajunen, L. *Mol. Phys.* **1980**, *39*, 715.
(30) Bebout, D. C.; Bush, J. F., II; Crahan, K. K.; Kastner, M. E.; Parrish, D. A. *Inorg. Chem.* **1998**, *37*, 4641−4646.
(31) For examples see: (a) Lipton, A. S.; Mason, S. S.; Myers, S. M.; Reger, D. L.; Ellis, P. D. *Inorg. Chem.* **1996**, *35*, 7111. (b) Reger, D. L.; Myers, S. M.; Mason, S. S.; Darensbourg, D. J.; Holtcamp, M. W.; Reibenspies, J. H.; Lipton, A. S.; Ellis, P. D. *J. Am. Chem. Soc.* **1995**, *117*, 10998.
(32) For examples see: (a) Santos, R. A.; Harbison, G. S. *J. Am. Chem. Soc.* **1994**, *116*, 3075. (b) Natan, M. J.; Millikan, C. F.; Wright, J. G.; O'Halloran, T. V. *J. Am. Chem. Soc.* **1990**, *112*, 3255.